HHS Public Access

Author manuscript

Alzheimers Dement. Author manuscript; available in PMC 2024 September 01.

Published in final edited form as:

Alzheimers Dement. 2023 September ; 19(9): 4110–4126. doi:10.1002/alz.13118.

Blood Tau-PT217 contributes to the anesthesia/surgery-induced delirium-like behavior in aged mice

Jing Lu, M.D., Ph.D.[1,2], **Feng Liang, M.D., Ph.D.**[2], **Ping Bai, Ph.D.**[3,4], **Chenghao Liu, Ph.D.**[2,5], **Miao Xu, M.D., Ph.D.**[2,6], **Zhengwang Sun, Ph.D.**[2], **Wenjie Tian, M.D., Ph.D.**[7,8], **Yuanlin Dong, M.D., M.S.**[2], **Yiying Zhang, M.D., Ph.D.**[2], **Qimin Quan, Ph.D.**[9], **Ashok Khatri, M.S.**[10], **Yuan Shen, M.D., Ph.D.**[2,11,12], **Edward Marcantonio, M.D., M.S.**[13], **Gregory Crosby, M.D.**[14], **Deborah Culley, M.D.**[15], **Changning Wang, PhD**[4], **Guang Yang, Ph.D.**[16,*], **Zhongcong Xie, M.D., Ph.D.**[2,*]

[1]Department of Anesthesiology, Sichuan Academy of Medical Sciences & Sichuan Provincial People's Hospital, Chengdu, Sichuan, 610072, China

[2]Geriatric Anesthesia Research Unit, Department of Anesthesia, Critical Care and Pain Medicine, Massachusetts General Hospital and Harvard Medical School, Charlestown, MA, 02129, United States

[3]Targeted Tracer Research and Development Laboratory, Precision Medicine Key Laboratory of Sichuan Province & Precision Medicine Center, West China Hospital, Sichuan University, Chengdu, Sichuan, 610041, China

[4]Athinoula A. Martinos Center for Biomedical Imaging, Department of Radiology, Massachusetts General Hospital and Harvard Medical School, Charlestown, MA, 02129, United States

[5]Chinese Academy of Sciences, Institute of Automation, Beijing, 100080, China

[6]Department of Anesthesiology, the First Affiliated Hospital, Sun Yat-sen University, Guangzhou, Guangdong, 510120, China

[7]Department of Cardiology, Sichuan Academy of Medical Sciences & Sichuan Provincial People's Hospital, Chengdu, Sichuan, 610072, China

[8]Cardiovascular Research Center and Cardiology Division of the Department of Medicine, Massachusetts General Hospital and Harvard Medical School, Charlestown, MA, 02129, United States

[9]NanoMosaic, Inc., Woburn, MA, 01801, United States

[*]Address correspondence to 1. Zhongcong Xie, M.D., Ph.D., Professor of Anesthesia, Geriatric Anesthesia Research Unit, Department of Anesthesia, Critical Care and Pain Medicine; Massachusetts General Hospital and Harvard Medical School; 149 13th Street, Room 4310; Charlestown, MA 02129-2060. (T) 617-724-9308; (F) 617-643-9277; zxie@partners.org; 2. Guang Yang, Ph.D., Associate Professor of Anesthesia, Department of Anesthesiology Columbia University Irving Medical Center New York, NY 10032. gy2268@cumc.columbia.edu.

Conflicts: Dr. Zhongcong Xie provides consulting services to Shanghai 9th and 10th hospitals, Baxter (invited speaker), and NanoMosaic in last 36 months. Dr. Qimin Quan is an employee of NanoMosaic but was not involved in data acquisition, analysis, and interpretation of the present study. All the authors declare no competing interests in the present study.

Consent Statement. The study did not include any human subjects. Therefore, it is not necessary to include informed consent.

[10]Endocrine Unit, Massachusetts General Hospital and Harvard Medical School, Boston, MA, 02129, United States

[11]Anesthesia and Brain Research Institute, Tongji University School of Medicine, Shanghai, 200092, China

[12]Mental Health Center affiliated to Shanghai Jiao Tong University School of Medicine, Shanghai, 200092, China

[13]Divisions of General Medicine and Primary Care and Gerontology, Department of Medicine, Beth Israel Deaconess Medical Center and Harvard Medical School, Boston, MA, 02115, United States

[14]Department of Anesthesiology, Brigham & Women's Hospital and Harvard Medical School, Boston, MA, 02115, United States

[15]Department of Anesthesiology and Critical Care, Perelman School of Medicine, University of Pennsylvania Health System, Philadelphia, PA, 19104, United States

[16]Department of Anesthesiology, Columbia University Medical Center, New York, NY, 10032, United States.

Abstract

INTRODUCTION: Blood phosphorylated Tau at threonine 217 (Tau-PT217) is a newly-established biomarker for Alzheimer's disease and postoperative delirium in patients. However, the mechanisms and consequences of acute changes in blood Tau-PT217 remain largely unknown.

METHODS: We investigated the effects of anesthesia/surgery on blood Tau-PT217 in aged mice, and evaluated the associated changes in B cell populations, neuronal excitability in anterior cingulate cortex, and delirium-like behavior using PET imaging, nanoneedle technology, flow cytometry, electrophysiology, and behavioral tests.

RESULTS: Anesthesia/surgery induced acute increases in blood Tau-PT217 via enhanced generation in the lungs and release from B cells. Tau-PT217 might cross blood-brain barrier, increasing neuronal excitability and inducing delirium-like behavior. B cell transfer and WS635, a mitochondrial function enhancer, mitigated the anesthesia/surgery-induced changes.

DISCUSSION: Acute increases in blood Tau-PT217 may contribute to brain dysfunction and postoperative delirium. Targeting B cells or mitochondrial function may have therapeutic potential for preventing or treating these conditions.

Keywords

Tau; Tau phosphorylation; Tau-PT217; anesthesia; surgery; delirium

2. Background.

Postoperative delirium is one of the most common postoperative complications in older patients [1], and is associated with postoperative complications [2], extended hospital stays [3], a higher chance of institutional discharge [4, 5], and increased morbidity [5-8]

and mortality [9, 10]. The annual healthcare costs in the United States attributable to postoperative delirium are approximate $32.9 billion [11]. Moreover, there is a strong bidirectional association between Alzheimer's disease (AD), AD Related Dementias (ADRD), and delirium [12]. Specifically, patients with underlying ADRD are 2.5 to 4.7 times more likely to develop delirium, and patients with delirium face a 12.5-fold increased incidence of newly diagnosed ADRD [4, 13-15]. However, the underlying mechanism of postoperative delirium remains largely unclear.

While Tau, a microtubule-associated protein, is predominantly found inside neurons [16-18], it is also present in peripheral organs [18, 19]. A recent study by Balczon et al. showed that the capillaries of rat lungs expressed endothelial Tau which could be detected by tomato lectin [20]. Moreover, administration of amyloid and Tau immunopurified from rat blood led to cognitive impairment in the recipient rats [20]. These data suggest that non-brain Tau can cause neuronal dysfunction and neurobehavioral deficits.

Tau protein undergoes many posttranslational modifications, including acetylation and phosphorylation [21]. Hyperphosphorylated Tau is one of the pathological hallmarks of AD and dementia [18, 22, 23]. For example, Tau phosphorylated at threonine 217 (Tau-PT217) and 181 (Tau-PT181) are the newly identified AD plasma biomarkers [24-32]. In AD patients, the rise of plasma Tau-PT217 amounts has been observed at the early preclinical stage of disease when insoluble Tau aggregates are not yet detected by Tau positron emission tomography [31]. Employing nanoneedle technology, an ultra-sensitive method to detect proteins, recent clinical studies demonstrated that preoperative plasma Tau-PT217 and Tau-PT181 are biomarkers for postoperative delirium [33] and anesthesia/surgery was associated with increases in plasma Tau-PT217 and Tau-PT181 amounts [34] in patients. However, despite extensive research on chronic changes in Tau metabolism, acute changes in blood Tau-PT217 are still poorly understood.

Whereas Tau binds to microtubules, the reduction of Tau does not change axonal transport, which critically depends on microtubules, in cultured primary neurons [35] or mouse optic nerve axons in vivo [36]. Rodents [37-42] and nonhuman primates [43, 44] well tolerate the genetic ablation of Tau. Other studies suggest that Tau can regulate many signaling pathways (reviewed in [21]), and enable neural network dysfunction and behavioral abnormalities caused by other pathogenic drivers in models of autism, depression, epilepsy, and stroke [37-39, 43-46]. Moreover, it is unknown whether anesthesia/surgery-induced delirium-like behavior in aged mice may involve acute increases in amounts of blood Tau-PT217, Tau-PT181 or other phosphorylated Tau proteins.

A recent study demonstrated that AD transgenic (Tg) mice had higher amounts of activated B cells in the cervical lymph node than wild-type (WT) mice had, and reductions in circulating B cells could decrease immunoglobulin deposits in the brain and prevent the progress of AD-like symptoms in the AD Tg mice [47]. However, other studies showed that AD patients had reduced B cells in blood [48, 49]. We, therefore, hypothesized that anesthesia/surgery induced behavioral changes in mice also via altering blood B cell number.

Combining PET imaging, nanoneedle technology, electrophysiology, and other methods, we demonstrated that anesthesia/surgery increased blood Tau-PT217 amounts potentially via increasing its generation in the lungs and releasing its binding from blood B cells. Administration of exogenous B cells from healthy mouse donors, or WS635, a non-immunosuppressive inhibitor of cyclophilin D and mitochondrial function enhancer [50, 51], attenuated the anesthesia/surgery-induced increases in Tau-PT217 measured in both blood and brain, restored the action potential firing rate in the slices of the anterior cingulate cortex (ACC), and mitigated the postoperative delirium-like behaviors in aged mice.

3. Methods.

3.1 Mice and treatments

The Standing Committee on Animals approved the animal protocol at Massachusetts General Hospital, Boston, MA (Protocol number: 2006N000219). All experiments were performed per the National Institutes of Health guidelines and regulations. Efforts were made to minimize the number of animals used. The manuscript was written according to ARRIVE guidelines. We used aged (18 months old) wild-type (WT) C57BL/6J female mice obtained from the National Institute on Aging (Bethesda, MD), female adult mice (3 months old, Jackson Lab, Bar Harbor, ME), and female Tau knockout (KO) mice (3 months old, Strain#: 007251, Jackson Lab) in the study. We only used female mice in the current studies because our previous studies showed that the female mice were more vulnerable to the development of cognitive impairment following anesthesia/surgery [52]. All mice were placed in the animal facility to adapt (12:12 h light: dark cycle with food and water available ad libitum) for three days before the study. The mice were randomly assigned into different groups by weight: (1) control condition plus vehicle treatment; (2) control condition plus anesthesia/surgery; (3) B cells or WS635 plus control condition; and (4) B cells or WS635 plus anesthesia/surgery. We determined the behavior of mice 6 hours after the anesthesia/surgery. Thus, conceptually, the studies aimed to determine the postoperative delirium of the perioperative neurocognitive disorder according to the new Recommendations for the Nomenclature of Cognitive Change Associated with Anesthesia and Surgery-2018 [53].

3.2 Anesthesia/surgery

Mice in the anesthesia/surgery group had a simple laparotomy under isoflurane anesthesia using the methods described in our previous studies [54-56] with a modification by using 40% oxygen. Specifically, we anesthetized each mouse using 1.4% isoflurane in 40% oxygen in a transparent acrylic chamber. We moved the mouse out of the chamber fifteen minutes after the induction. Isoflurane anesthesia was maintained via a cone device, and one 16-gauge needle was inserted into the cone near the nose of the mouse to monitor the concentration of isoflurane. We then made a longitudinal midline incision from the xiphoid to the 0.5-centimeter proximal pubic symphysis on the skin, abdominal muscles, and peritoneum. We sutured the incision layer by layer with 5-0 Vicryl thread. We applied EMLA cream (2.5% lidocaine and 2.5% prilocaine) to the incision site at the end of the procedure. The procedure for each mouse usually lasted about 10 minutes. We put the mouse back into the anesthesia chamber to continue receiving the rest of the anesthesia consisting of 1.4% isoflurane in 40% oxygen for up to two hours. We maintained the rectal temperature

of the mice at 37 ± 0.5 °C during the anesthesia/surgery using the D.C. Temperature Control System (FHC, Bowdoinham, Maine). After recovering from the anesthesia, we returned the mice to their home cage with food and water available *ad libitum*. The mice in the control group were placed in their home cages with room air for two hours, which is more clinically relevant that people without anesthesia/surgery breath room air. The blind procedure was not possible in the studies because of the appearance of the abdominal wound in the mice.

3.3 WS635 treatment

WS635 (sodium taurocholate hydrate) was provided by Waterstone Pharmaceutical company (Wuhan, China). WS635 dissolved in vehicle (0.2 ml corn oil with 10% DMSO), each of the mice was injected with WS635 solution in the dose of 40 mg/kg in 0.2 ml through intraperitoneal route at 30 minutes before the anesthesia/surgery.

3.4 Isolation of B cells and T cells from blood

Blood samples were harvested from aged mice. B cells and T cells were isolated from leukocytes using EasySep™ Mouse B cell Isolation Kit (Cat#19854, Stemcell™) and EasySep™ Mouse T cell Isolation Kit (Cat#19851, Stemcell™). Invitrogen™ CellTracker™ Green CMFDA Dye (1:1000 Cat# C7025, Invitrogen™, Waltham, MA) was incubated with purified B cells and T cells for 30 minutes. After washing with PBS, cells in the dishes were incubated with Cy3-link-peptide at 37 °C with 5% CO2 for 20 minutes. After incubation, cells were rewashed with PBS, and culture media were replaced with RPMI 1640 Medium (Cat# 11835030, ThermoFisher Scientific). Before confocal examinations.,4 μL of NucBlue Live ReadyProbes reagent (Hoechst 33342) (Cat# R37605, Invitrogen™) were incubated with cells for an additional 10 minutes for nuclear staining.

3.5 B cell treatment

We collected B cells from splenocytes of 3-month-old female mice using a Mouse B cell Isolation Kit (Cat#19854, Stemcell™ Cambridge MA). Mouse spleen was mashed through a 70 μm nylon mesh in 10 ml PBS. The spleen cell suspension was incubated with red blood cell lysis buffer (Cat# 555899, B.D. Bioscience) at room temperature for 10 minutes. We injected 2 X 10^6 B cells in 200 uL sterile PBS into each of the 18-month-old mice via the tail vein 30 minutes prior to anesthesia/surgery, immediately after collecting the cells from the spleen.

3.6 Confocal microscopy for live cell imaging

B cells and T cells collected from blood were cultured in 35-mm glass-bottom dishes (Cat#:801002 NEST Scientific Inc. Woodbridge, NJ) before observations after staining with 5-chloromethylfluorescein diacetate (CMFDA), NucBlue and Cy3. Cells were imaged with a PLAPON 60 X oil-immersion objective and 405 nm (blue), 488nm (green), and 594 nm (red) channels after incubation with Tau-PT217 peptide or Tau peptide (1 ug/200 ul). The Olympus FV1000 confocal microscopy system (Cat#: F10PRDMYR-1, Olympus, USA) and FV1000 software were used to acquire live cell images.

3.7 Behavior tests

There is no ideal animal model to study delirium. Our previous studies used the Confusion Assessment Methods (CAM)-in-Mice model, including a battery of behavioral tests, to determine the delirium-like behavior in mice [54, 56-58]. We performed the behavioral tests in 3 mice per group at one time and finished them within 50 minutes, representing the certain features of clinical evaluation of delirium in patients. The battery of behavioral tests included the buried food test, Y maze test, and open field test to capture certain domains mimicking the delirium-like behavior in mice. The composite Z-scores to present the postoperative delirium-like behavior of each mouse were calculated using the methods described in previous studies [54, 59]. Specifically, the Z score was calculated using the formula described by Moller et al.: Z = [ΔX Anesthesia/surgery – MEAN(ΔX) control]/ standard deviation (SD)(ΔX) control [59]. In the formula, ΔX control was the change score of mice in the control group at 6 hours after the control condition minus the score at the baseline; ΔX Anesthesia/surgery was the change score of mice in the anesthesia/surgery group at 6 hours after the anesthesia/surgery minus the score at baseline; MEAN(ΔX) control was the mean of ΔX control, and SD (ΔX) control was the standard deviation of ΔX control. We also used the method for calculating a composite Z score in patients [60, 61] to determine a composite Z score for each of the mice. Specifically, the composite Z score for the mouse was calculated as the sum of the values of 6 individual Z score (latency to eat food, time spent in the center, latency to the center, freezing time, entries in novel arm, and duration in novel arm) normalized with SD for that sum in the controls. Given that the reduction (rather than increase) in time spent in the center, the freezing time (open field test), the reduction in duration, and entries in the novel arm (Y maze test) indicate impairment of the behavior, we multiplied the Z score values representing these behaviors by −1 prior to calculating the composite Z score using these values in the mice.

3.8 Harvest of mice brain, lung, and spleen tissues

Mice were euthanized with CO2. We then harvested mouse lungs, hippocampus, and cortex at 6 hours after the anesthesia/surgery for the Western blot analysis.

3.9 Collection of blood, brain, and lungs of mice

Mice were euthanized with CO2. We exposed the heart and collected blood at 3 and 6 hours after the anesthesia/surgery with a one microliter syringe into an EDTA tube for the flow cytometry and nanoneedle studies. We harvested mouse lungs, hippocampus, and cortex at 30 minutes, 3 hours and 6 hours after the anesthesia/surgery for the Western blot analysis.

3.10 Injection of WT mouse blood to Tau KO mice

We harvested 600 ul intracardial blood from a WT aged mouse that received the control condition and another WT aged mouse that received the anesthesia/surgery. The blood samples were centrifuged at 2000 g for 10 minutes, and the plasma was collected and placed into a tube. We then injected 200 ul of the plasma into each of the two Tau KO mice via the tail vein. Finally, we harvested the brain tissues of the two Tau KO mice and measured Tau-PT217 amounts in the harvested brain tissues using nanoneedle at 6 hours after the injection.

3.11 Positron emission tomography (PET) study of mice.

The Standing Committee on Animals approved the animal protocol of the PET study at Massachusetts General Hospital, Boston, MA (Protocol number: 2020N000042). The general procedure for rodent PET/CT imaging studies was described previously [62, 63]. Briefly, aged mice (18 months old) were arranged in a carrier under anesthetized with 1% isoflurane (Patterson Vet Supply, Inc., Greeley, CO, USA) and 2 L/min medical oxygen for the duration of scanning. Mice were injected with the [^{18}F]Flortaucipir (3.7– 7.4 Mbq per animal, prepared in house prior to each PET scan) via a tail vein catheterization before PET acquisition. Four mice were scanned by PET for two hours on the day before the anesthesia/surgery as the baseline. On the day of anesthesia/surgery, the mice had two hours of anesthesia/surgery, recovered for one hour, and were scanned by PET for two hours. Dynamic PET acquisition lasted two hours, followed by 10 minutes of computed tomography (CT) for anatomic co-registration. PET data were reconstructed using a 3D-MLEM method, resulting in full width at a half-maximum resolution of 1 mm. These files were imported and analyzed using AMIDE44 (a medical imaging data examiner) software (an open-source software, Los Angeles, CA, USA) and PMOD (PMOD 4.01, PMOD Technologies Ltd., Zurich, Switzerland). The dynamic PET data were collected, and the corresponding images were reconstructed by the 3DMLEM method, resulting in full width at a half-maximum resolution of 1 mm. Volumes of interest (VOIs) were generated manually in the form of spheres under the guide of high-resolution CT structural images. Time-activity curves (TACs) were exported as decay-corrected activity per unit volume.

3.12 Measurement of Tau-PT217 by nanoneedles

Blood samples were centrifuged at 2000 g for 10 minutes, and plasma supernatant was collected into an EDTA tube. The Tau-PT217 was measured by nanoneedle (NanoMosaic, Waltham, MA) as described in our previous studies [33, 34]. Blank nanoneedle chips were supplied by NanoMosaic. Five μg/ml capture antibody was incubated with the nanoneedle chip overnight. It was then washed in PBS and incubated in the blocking solution for 1 hour. Five μL of plasma samples were diluted 2 X into the dilution buffer provided by NanoMosaic. The diluted sample was incubated on the chip for 2 hours. After washing, 0.5 ug/ml detection antibody was incubated on the chip. We used phospho-specific antibody to Tau-PT217 (Cat#44-744, ThermoFisher) as the detection antibody. We used Tessie™ instrument (NanoMosaic) to image the chip and the software provided by NanoMosaic to analyze the colors of all nanoneedles and reported the percentage of the color-shifted number of nanoneedles. The protein concentrations were reported in relative units specific to the nanoneedle technology (i.e., Nano Unit).

3.13 Flow cytometry

Single-cell suspensions from blood were prepared. Whole blood samples were incubated with red blood cell lysis buffer (Cat:555899, BD Bioscience, Woburn, MA) for 10 minutes at room temperature to allow the lysis of red blood cells, washed with flow cytometry stain buffer (Cat#554656, BD Bioscience) twice, and spun down at 500 g X 5 minutes at 4°C. Leukocytes were resuspended in 200 μL staining buffer. To perform single-cell suspensions, the cells were processed, and their viability was assessed using the eBioscience™ Fixable

Viability Dye eFluor™ 506 (Cat# 65086614, Invitrogen, Waltham, MA). After staining, the cells were washed with FACS buffer. Nonspecific binding to Fc receptors was blocked by incubation with a mouse FcR Blocking Reagent (Cat#130092575, Miltenyi Biotec, Cambridge, MA) at 4 °C for 15 minutes. Cells were washed and proceeded to stain with the following antibodies: anti-mouse CD45 APC/Cyanine7 (Cat#103116, Biolegend, Dedham, MA), anti-mouse Ly-6G BUV395(Cat#563978, BD Biosciences), anti-mouse CD3 APC (CAT#100236, Biolegend), anti-mouse CD11b BV421 (Cat#101236, Biolegend), anti-mouse CD19 PE/Cyanine7 (Cat#152408, Biolegend). MitoProbeTM TMRM Kit (Cat#M20036, ThermoFisher Scientific, Waltham, MA) was used to detect the amounts of TMRM-positive B cells. Samples were run on BD LSRFortessa™ with a UV laser cell analyzer. Results were analyzed by using FlowJo software 10.7.2.

3.14 Western blot

The harvested brain tissues were lysed using lysis buffer, immunoprecipitation buffer (Tissue Protein Extraction Reagent, Cat# 78501; ThermoFisher Scientific), protease and phosphatase inhibitor cocktail (Cat# A32959; ThermoFisher Scientific). The harvested lung tissues were lysed using Thermo Scientific™ RIPA Lysis and Extraction Buffer (Cat# 89900; Thermo Scientific, Waltham, MA, USA) plus protease and phosphatase inhibitor cocktail (Cat# A32959; ThermoFisher Scientific). Lysates were collected and centrifuged for 20 minutes at 16000 g at 4°C. Total protein amounts were quantified using the Pierce™ protein assay kit (Cat# 23225, ThermoFisher Scientific). Total Tau and Tau-PT217 protein amounts were detected with anti-Tau 46 antibody (Cat# T9450, 1:1000; Sigma-Aldrich, St Louis, MO) and Phospho-tau-Ser217 antibody (Cat# 44744, 1:500; ThermoFisher Scientific) with incubation at 4 °C overnight. Antibodies β-actin (Cat# A5441, 1:5000; Sigma-Aldrich) and GAPDH (Cat# 2118S,1:5000, Cell Signaling Technology, Danvers, MA) served as the loading control. Images were taken in a Universal Hood II machine with corresponding ImageLab software (Bio-Rad, Hercules, CA). We quantified Western blots in two steps. First, we used β-Actin or GAPDH amounts to normalize (e.g., determine the ratio of Tau to β-Actin amount) and control for loading differences in the total protein amount. Second, we presented protein amount changes in mice in the treatment group as a percentage of those in the control group. One hundred percent of protein amount changes referred to control amounts for comparison of experimental conditions.

3.15 Peptide Synthesis, purification, and analysis

Peptides were synthesized on an automated robotic peptide synthesizer (Intavis, Model Multipep) by using Standard Fmoc solid-phase chemistry [64]. Phospho-Thr was incorporated using Fmoc-Phospho-Thr(OBzl)-O.H. Rink amide resin with MBHA linker was used to generate peptides containing C-terminal carboxamides. Subsequent amino acids were coupled using optimized (to generate peptides containing more than 90% of the desired full-length peptides) cycles consisting of Fmoc removal (deprotection) with 25% Piperidine in NMP followed by coupling of Fmoc-AAs using HBTU/HOBt/DIEA activation. Each deprotection or coupling was followed by several washes of the resin with DMF to remove excess reagents. After the peptides were assembled and the final Fmoc group removed, peptide resins were washed with dimethylformamide, dichloromethane, and methanol three times each and air dried. Peptides were cleaved from the solid support and deprotected using

odor free cocktail (TFA/triisopropyl silane/water/DODT; 94/2.5/2.5/1.0 v/v) for 2.5 hours at room temperature [65]. Peptides were precipitated using cold methyl tertiary butyl ether (MTBE). The precipitate was washed two times in MTBE, dissolved in a solvent (0.1% trifluoroacetic acid in 30%Acetonitrile/70%water), followed by freeze-drying. Purifications were performed using preparative reverse-phase HPLC. Microbore HPLC and Matrix characterized peptides Assisted Laser Desorption/Ionization Mass Spectrometry (MALDI-MS). Cy3® Conjugation Kit (Fast) - Lightning-Link® (ab188287, Abcam, Cambridge, MA) provides a procedure for labeling the peptide with Cy3®. The synthesized Tau-PT217 peptide consists of 14 amino acids and includes a portion of the PT217 sequence. The peptide sequence with Tau-PT217 is PGSRSRTPSLP$_P$TPP, while the sequence without Tau-PT217 is PGSRSRTPSLPTPP.

3.16 Electrophysiology to measure action potential firing rate in ACC slices

Aged mice (18 months old female mice) were intraperitoneally injected with WS635 dissolved in a vehicle or vehicle only. Half an hour later, mice from the experimental group went through the anesthesia/surgery. The control animals were left untreated. 6 hours later, the animals were sacrificed for electrophysiology recording. The mice were deeply anesthetized with 10 ml/kg body weight of 9 mg/ml ketamine and 1 mg/ml xylazine, and perfused with an ice-cold oxygenated cutting solution containing (in mM): 100 N-methyl-D-glucamine (NMDG), 3 KCl, 1 NaH2PO4, 25 NaHCO3, 20 HEPES, 2 Thiourea, 3 Sodium Pyruvate, 12 N-acetyl-L-cysteine, 6 MgCl2, 0.5 CaCl2, 5 Sodium Ascorbate, 10 Glucose (pH: 7.25–7.4, adjusted using HCl). Brain slices with 300 μM thick containing the mouse ACC were cut on a vibratome and then recovered in the cutting solution at 32-34 °C for 15 minutes. The slices were then moved to oxygenated recording artificial cerebrospinal fluid (ACSF) containing (in mM): 126 NaCl, 3 KCl, 1 NaH2PO4, 25 NaHCO3, 2 MgCl2, 2 CaCl2, 10 Glucose. The slices were perfused with oxygenated recording ACSF at room temperature during recordings. Whole-cell recording pipettes (3–7 MW) were filled with an internal solution containing (in mM): 100 K-gluconate, 20 KCl, 10 HEPES, 4 Mg-ATP, 0.3 Na-GTP, 10 Na-phosphocreatine, and 0.1% biocytin. Recordings of the action potential firing rate were amplified (Multiclamp 700B, Molecular Devices, San Jose, CA) and digitized at 10 kHz using Digidata 1332A (Molecular Devices) under the control of Clampex (Molecular Devices). All recordings were done in the current clamp. The liquid junction potential was not compensated. Neurons with high series resistance (>20 MW current clamp) or membrane potentials that changed by >10 mV were excluded. A series of step currents were applied, and the action potential was recorded.

3.17 Statistics and Reproducibility

Based on our previous studies, we determined that 10 - 12 mice per group for the behavioral studies and 4 - 6 samples per group for the biochemistry studies would provide sufficient statistical power. We present data from biochemistry studies and behavior studies as mean ± standard deviation (SD). There were no missing data for variables of the behavioral tests. Two-way ANOVA (analysis of variance) and post-hoc analysis with Bonferroni were used to determine the interactions and differences between groups (e.g., control versus anesthesia/surgery) and treatments (e.g., vehicle versus WS635). Student's t-test was used to determine the differences in two-group comparison when data passed a normality test. One-

way ANOVA and post-hoc analysis with Bonferroni were used to determine the differences between groups. $P < 0.05$ was considered statistically significant, and significance testing was two-tailed. Adjusted Bonferroni correction *P*-values were calculated by dividing real *P*-values with experiment size, and adjusted *P*-values are reported in the manuscript. Statistical analysis was conducted using GraphPad Prism software (version 8.0) and SPSS statistics software (version 21.0).

4. Results.

4.1 Anesthesia/surgery increased Tau-PT217 amounts in the lungs, blood, and brain tissues of aged mice.

Our clinical studies revealed that preoperative blood Tau-PT217 concentration was a predictor of postoperative delirium [33], and anesthesia/surgery was associated with increased blood Tau-PT217 amounts in patients [34]. We, therefore, conducted a preclinical study to investigate the mechanism by which blood Tau-PT217 contributed to delirium-like behavior in aged mice after anesthesia/surgery. We found that anesthesia/surgery increased Tau-PT217 amounts in the lungs, blood, and brain tissues of aged mice, which was consistent with our clinical findings. PET imaging in mice (S-Video. 1) showed that the anesthesia/surgery increased the amounts of tracer representing Tau-PT217 in the lungs (Fig. 1a, 1b, and 1c, S-Fig. 1a and 1b) and blood (Fig. 1a, 1d, and 1e) of aged mice compared to baseline, as evidenced by increases in standard uptake value (SUV) or standard uptake value ratio (SUVR) of the tracer. PET imaging of the brain also demonstrated increased amounts of tracer representing Tau-PT217 in whole brain tissues (Fig. 1f, 1g, and 1h, S-Fig. 1c and 1d), cortex (Fig. 1f, 1i, and 1j) and hippocampus (Fig. 1f, 1k, and 1l) of aged mice. Notably, anesthesia/surgery-induced increases in Tau-PT217 occurred earlier in the blood and lungs of aged mice than in brain tissues (S-Fig. 1e). Between 30 to 120 minutes after the anesthesia/surgery, the amounts of Tau-PT217 appeared to be higher in lungs than in brain tissues (S-Fig. 1f).

We validated these findings using nanoneedle (Fig. 2a and 2b) and Western blotting techniques. Nanoneedle showed increased amounts of blood Tau-PT217 in the aged mice 3 and 6 hours after the anesthesia/surgery compared to the control condition (Fig. 2c). Western blot analysis confirmed that the amounts of Tau-PT217 in the cortex (Fig. 2d and 2e) and hippocampus (Fig. 2f and 2g) of aged mice were increased 6 hours after the anesthesia/surgery compared to the control condition. Interestingly, greater increases of Tau-PT217 amounts were observed in the lungs than in the cortex 30 minutes after the anesthesia/surgery (Fig. 2h, 2i, and 2j), whereas more increases of Tau-PT217 amounts were detected in the cortex than in the lungs 3 hours after the anesthesia/surgery (Fig. 2k, 2l, and 2m). There were no significant changes in total Tau amounts in both cortex and lungs (Fig. 2k, 2l, and 2m). These data suggest that the anesthesia/surgery may increase Tau-PT217 amounts in the lungs earlier than in the cortex of aged mice. By contrast, neither 40% oxygen nor 1.4% isoflurane plus 40% oxygen significantly altered the amounts of Tau-PT217 in blood, cortex, and hippocampus of aged mice (S-Fig. 2a-e).

To test whether blood Tau-PT217 may spread to the brain parenchyma, we collected plasma from aged wild-type mice with or without anesthesia/surgery and administered the plasma

to a Tau knockout (KO) mice (S-Fig. 2f). Brain tissue analysis conducted six hours after plasma treatment revealed higher levels of Tau-PT217 in Tau KO mice that received plasma from mice subjected to anesthesia/surgery, compared to the control group (S-Fig. 2g), suggesting that blood Tau-PT217 may enter the brain of mouse or induce an increase in brain Tau-PT217 amounts.

4.2 Anesthesia/surgery decreased blood B cells in aged mice.

Previous studies have demonstrated a relationship between changes in blood B cells and the development of AD dementia [47-49]. Thus, we sought to investigate whether anesthesia/surgery could induce significant changes in B cell amounts in aged mice. Using flow cytometry analysis (S-Fig. 3), we observed a marked decrease in the number of blood B cells in aged mice 6 hours after anesthesia/surgery compared to the control condition (Fig. 3a and 3b). Additionally, we found that the mitochondrial membrane potential, as represented by the amounts of tetramethylrhodamine methyl ester (TMRM), was significantly lower 6 hours after anesthesia/surgery compared to the control condition (Fig. 3c and 3d). These results suggest that the anesthesia/surgery may reduce the number of B cells by compromising their mitochondrial function.

In light of the findings that anesthesia/surgery decreased blood B cell number and increased blood Tau-PT217 amounts in the aged mice, we aimed to investigate the potential interaction between B cells and Tau-PT217. Since commercial recombinant Tau-PT217 was not available, we synthesized 14 amino acid peptide containing a portion of Tau-PT217 (Tau-PT217 peptide) and examined its interaction with B cells *in vitro*. Confocal imaging clearly revealed that the Tau-PT217 peptide specifically bound to B cells (first row of Fig. 3e and S-Video 2), but not to T cells (second row of Fig. 3e). Furthermore, the control Tau peptide, which had an identical amino acid sequence to the Tau-PT217 peptide but lacked phosphorylation of threonine 217, did not bind to B cells (third row of Fig. 3e). These results suggest that blood B cells can bind to Tau-PT217, potentially serving as a cellular mechanism to buffer acute increases in Tau-PT217 amounts in the blood of aged mice.

4.3 Treatment with B cells attenuated the anesthesia/surgery-induced changes in aged mice.

To investigate whether B cells can restore the blood B cell number and attenuate the anesthesia/surgery-induced increase in blood Tau-PT217 levels and delirium-like behavior, we treated the aged surgical mice with exogenous B cells harvested from donor mice 30 minutes before the anesthesia/surgery (Fig. 4a). Six hours after adoptive cell transfer, flow cytometry analysis showed that the number of blood B cells in recipient mice was restored to levels comparable to those in control mice with vehicle treatment (Fig. 4b and 4c). Additionally, B cell treatment attenuated the anesthesia/surgery-induced increases in blood Tau-PT217 levels (Fig. 4d) and the ratio of Tau-PT217/Tau in the cortex (Fig. 4e and 4f). B cell treatment also mitigated the anesthesia/surgery-induced delirium-like behavior in the aged mice (Fig. 4g) and attenuated the anesthesia/surgery-induced increases in Z score, which represents delirium-like behavior (Fig. 4h and S-Fig. 4). These findings suggest that anesthesia/surgery may increase blood Tau-PT217 amounts by reducing blood B cell numbers, which can lead to delirium-like behaviors in aged mice, and that treatment with

B cells can restore blood B cell numbers and mitigate these anesthesia/surgery-induced changes.

4.4 Treatment with WS635 attenuated the anesthesia/surgery-induced changes in aged mice.

To investigate whether the anesthesia/surgery-induced reduction in blood B cell numbers was due to decreased mitochondrial function [66], we examined whether WS635, a non-immunosuppressive inhibitor of cyclophilin D and mitochondrial function enhancer [50, 51], could attenuate the anesthesia/surgery-induced changes in blood, neuronal and behavioral changes in aged mice. As compared to treatment with vehicle, treatment with WS635 in the aged mice attenuated the anesthesia/surgery-induced decreases in blood B cell number (Fig. 5a and 5b), decreases in the mitochondrial function, e.g., mitochondrial membrane potential (represented by TMRM amounts), of the blood B cells (Fig. 5c and 5d), and increases in blood Tau-PT217 amounts (Fig. 5e). Immunoblotting of Tau-PT217 and Tau46 showed that the treatment of WS635 mitigated the anesthesia/surgery-induced increases in Tau-PT217/Tau ratio in the cortex of aged mice compared to the treatment of vehicle (Fig. 5f and 5g). The WS635 treatment mitigated the anesthesia/surgery-induced delirium-like behavior in the aged mice compared to the vehicle treatment (Fig. 5h and 5i, and S-Fig. 5).

We evaluated the effects of anesthesia/surgery on neuronal activity by measuring the action potential firing rate in the Anterior Cingulate Cortex (ACC) of aged mice through slice recording. We found that anesthesia/surgery increased the ACC neuronal excitability (the action potential firing rate) in the aged mice without pretreatment (Fig. 6a, 6b, and 6c) or the aged mice pretreated with corn oil, the vehicle of WS635 (Fig. 6d, 6e, and 6f). However, WS635 pretreatment attenuated the anesthesia/surgery-induced increase in ACC neuronal excitability in the aged mice (Fig. 6g, 6h, and 6i). These findings, along with the results of our biochemistry and behavioral studies, suggest that WS635 can mitigate the anesthesia/surgery-induced elevation of blood Tau-PT217, neuronal hyperexcitability, and delirium-like behavior in aged mice.

5. Discussion.

Anesthesia/surgery increased blood Tau-PT217 amounts by promoting its generation in lungs and releasing its binding from B cells, which in turn may enter brain and increase excitability of ACC neurons, resulting in postoperative delirium-like behavior in aged mice (Fig. 7). Anesthesia/surgery may reduce blood B cell number by impairing their mitochondrial function, thereby releasing B cell-bound Tau-PT217. Treatment with B cells or the mitochondrial function enhancer WS635 mitigated the anesthesia/surgery-induced changes (Fig. 7). These findings demonstrate the contribution of acute increases in blood Tau-PT217 to postoperative delirium pathogenesis, which provide insights into the upstream mechanism and downstream consequences of the acute change of Tau metabolism in blood. These results also have important translational implications and suggest potential strategies for preventing and treating postoperative delirium.

Tau protein is not exclusively found in neurons, but also in non-neuronal cells such as the lungs [20, 67]. A previous study demonstrated that plasma levels of Tau-PT217 were

independently associated with brain loads of both β-amyloid and Tau in patients [68]. In present study, we observed an increase in Tau-PT217 in lungs, blood, and brain tissues of aged mice following anesthesia/surgery (Fig. 1 and 2). Notably, the increase in Tau-PT217 occurred earlier in the lungs than in the brain tissues (Fig. 2h-2l and S-Fig. 1e and 1f), and Tau-PT217 might enter the brain of the mice (S-Fig. 2f and 2g). These findings suggest that the increased Tau-PT217 in the blood following anesthesia/surgery may enter the brain, leading to neuronal dysfunction. This conclusion is further supported by our observation that treatment with B cells or WS635 mitigated the anesthesia/surgery-induced increases of brain Tau-PT217 amounts, ACC neuronal excitability, and postoperative delirium-like behavior in aged mice.

At present, it is unclear whether the increased amounts of Tau-PT217 in the blood or brain are derived from the blood or brain. However, the aim of this study was to investigate whether the elevated levels of blood Tau-PT217 were responsible for postoperative delirium-like behavior in aged mice. The results revealed a correlation between changes in blood Tau-PT217 levels and postoperative delirium-like behavior in the aged mice. The future studies should develop antibodies that can differentiate between blood-derived and brain-derived Tau-PT217 in mice [69], and further define the contribution of blood and brain Tau-PT217 to the disorder.

Kim et al. reported that AD Tg mice had increased amounts of B1a and B1b cells, but decreased amounts of B2 cells, in the cervical lymph nodes compared to age- and sex-matched WT mice of the same strain [47]. Furthermore, depletion of B cells reduced the Aβ plaque burden and microglia activation in the hippocampus of AD Tg mice and improved AD symptoms, such as retarded locomotion, in the AD Tg mice [47].

The data from the present study suggest that anesthesia/surgery decreased the number of B cells in the blood (Fig. 3), and treatment with B cells attenuated the anesthesia/surgery-induced increase in blood Tau-PT217 amounts and delirium-like behaviors in aged mice (Fig. 4). However, the previous study differs from the present study in several aspects: (1) the use of AD Tg mice without environmental modifications versus aged WT mice that received anesthesia/surgery; (2) changes in B cell numbers in cervical lymph nodes versus blood; (3) increases in B1a and B1b cells but decreases in B2 cells versus a decrease in B cells; and (4) a chronic condition versus acute changes following anesthesia/surgery. Moreover, other studies have reported that AD patients have a lower number of B cells in their blood [48, 49], and treatment with B cells may improve AD neuropathogenesis and cognitive impairment in AD Tg mice [70]. Nevertheless, further studies are needed to determine the role of B cells in the pathogenesis of postoperative delirium.

The confocal *in vitro* studies demonstrated that B cells (Fig. 3e and S-Video 2) could specifically bind to the Tau-PT217 peptide, while T cells (Fig. 3e) did not. These findings suggest that B cells may act as a buffer or reservoir to mitigate the anesthesia/surgery-induced increases in blood Tau-PT217 levels by binding to Tau-PT217 in the blood. Since recombinant Tau-PT217 is not commercially available, this study only demonstrated the specific binding of B cells to the 14 amino acid Tau-PT217 peptide. Further studies will aim to generate recombinant Tau-PT217 and investigate the potential binding between the

recombinant Tau-PT217 and B cells. The B cell receptor, a transmembrane protein on the surface of B cells [71], may play a role in the binding between B cells and Tau-PT217. Future studies will also investigate this potential mechanism.

WS635, an analog of cyclosporine A, is a blocker of mitochondrial permeability pore (mPTP) opening [72, 73] but without immunosuppressive effects as cyclosporine A, another mPTP blocker [50, 51]. Our previous study showed that chronic treatment with WS635 attenuated anesthesia/surgery-induced cognitive impairment in mice [74]. In this study, we demonstrated that acute treatment with WS635 mitigated the anesthesia/surgery-induced mitochondrial dysfunction of B cells, which in turn attenuated the anesthesia/surgery-induced decreases in the amounts of blood B cells and increases of blood Tau-PT217 amounts, leading to lesser postoperative delirium-like behavior in the aged mice. These findings suggest that WS635 may be a potential therapeutic strategy to attenuate perioperative neurocognitive disorder, including postoperative delirium, delayed neurocognitive recovery, and neurocognitive disorder in patients. Future randomized clinical trials are needed to determine the efficacy and safety of WS635 in patients undergoing anesthesia and surgery.

Due to constraints of anti-tau antibody, including the cost and potential failures of treating neurological disorders [75], we did not assess the effects of Tau-PT217 antibody on postoperative delirium-like behavior in aged mice. Instead, we chose to reduce blood Tau-PT217 levels by administering WS635 or B cells, which effectively lowered Tau-PT217 levels and mitigated postoperative delirium-like behavior in aged mice, providing strong evidence of the involvement of Tau-PT217 in postoperative delirium. While we expect that Tau KO mice, as previously demonstrated in our studies [76], would not display postoperative delirium-like behavior, this result alone does not definitively establish the contribution of blood Tau-PT217 to the observed postoperative delirium-like behavior in aged mice.

There has been no ideal animal model to study postoperative delirium-like behavior [77]. Despite the need for an ideal animal model to study postoperative delirium-like behavior, our lab has developed an animal behavioral test battery. This battery includes natural behaviors such as buried food and an open-field test to evaluate attention and awareness, as well as a learned behavior test (Y maze) to assess cognition [54, 56-58, 78]. These tests evaluate behaviors in mice that rely on intact attention, organized thinking, and consciousness. Notably, we have demonstrated that aged mice display greater susceptibility to these behaviors after anesthesia/surgery compared to adult mice [56], which parallels the clinical observation of a higher incidence of POD in senior patients relative to adult patients.

The study has some limitations that warrant further investigation. First, the study did not investigate the potential age- and sex-dependent effects of blood Tau-PT217 on the development of postoperative delirium-like behavior in mice. Future studies should consider these factors to gain a more comprehensive understanding of the relationship between blood Tau-PT217 and postoperative delirium-like behavior. In future studies, it may also be valuable to further investigate the impact of anesthesia alone on the levels of Tau-PT217 in the blood and brain of aged mice. Second, the data obtained from the current study

could not definitively determine whether the transport of Tau-PT217 between blood and brain was passive or active. Additionally, it could not confirm whether brain Tau-PT217 was solely derived from blood or whether it was increased via different mechanisms, such as inflammation and neuroinflammation. Therefore, future research should focus on further investigating the roles of blood Tau-PT217, brain Tau-PT217, and delirium-like behavior. Overall, while the present study sheds light on the association between blood pTau and postoperative delirium in aged mice, there is still much to be learned about the complex mechanisms underlying this relationship.

6. Conclusion.

Our study demonstrated that anesthesia and surgery led to an acute increase in the levels of Tau-PT217 in the blood by promoting its generation in the lungs and releasing its binding from B cells. This increase in Tau-PT217 might then enter the brain and increase the excitability of ACC neurons, ultimately leading to delirium-like behaviors in aged mice. We found that treatment of B cells or WS635 could attenuate the anesthesia/surgery-induced increase in Tau-PT217 levels in the blood, ACC neuronal excitability, and delirium-like behaviors in aged mice. These findings suggest that changes in blood Tau-PT217 levels may contribute to the development of postoperative delirium in mice and may have implications for the development of targeted interventions to improve postoperative outcomes in older patients. Further studies are needed to better understand the underlying mechanisms and to determine the potential clinical relevance of these findings. Ultimately, this work may contribute to the development of new strategies for the prevention and treatment of postoperative delirium.

Supplementary Material

Refer to Web version on PubMed Central for supplementary material.

Acknowledgments:

These studies were performed in Massachusetts General Hospital and Harvard Medical School and are attributed to the Department of Anesthesia, Critical Care and Pain Medicine, Massachusetts General Hospital, and Harvard Medical School. WS635 was provided as a gift from Waterstone Pharmaceutical, Wuhan, China. The authors thank Dr. Jianren Mao at Massachusetts General Hospital for the use of electrophysiology device.

Funding Sources:

This research was supported by AG0041274 (Zhongcong Xie and Guang Yang), AG062509 (Zhongcong Xie) and AG070761 (Zhongcong Xie) from the National Institutes of Health, Bethesda, MD.

Reference

[1]. Vutskits L, Xie Z. Lasting impact of general anaesthesia on the brain: mechanisms and relevance. Nat Rev Neurosci. 2016;17:705–17. [PubMed: 27752068]

[2]. Inouye SK. Delirium in older persons. N Engl J Med. 2006;354:1157–65. [PubMed: 16540616]

[3]. Rudolph JL, Jones RN, Rasmussen LS, Silverstein JH, Inouye SK, Marcantonio ER. Independent vascular and cognitive risk factors for postoperative delirium. Am J Med. 2007;120:807–13. [PubMed: 17765051]

[4]. Witlox J, Eurelings LS, de Jonghe JF, Kalisvaart KJ, Eikelenboom P, van Gool WA. Delirium in elderly patients and the risk of postdischarge mortality, institutionalization, and dementia: a meta-analysis. JAMA. 2010;304:443–51. [PubMed: 20664045]

[5]. Martin BJ, Buth KJ, Arora RC, Baskett RJ. Delirium as a predictor of sepsis in post-coronary artery bypass grafting patients: a retrospective cohort study. Crit Care. 2010;14:R171. [PubMed: 20875113]

[6]. Koster S, Hensens AG, van der Palen J. The long-term cognitive and functional outcomes of postoperative delirium after cardiac surgery. Ann Thorac Surg. 2009;87:1469–74. [PubMed: 19379886]

[7]. Marcantonio ER, Flacker JM, Michaels M, Resnick NM. Delirium is independently associated with poor functional recovery after hip fracture. J Am Geriatr Soc. 2000;48:618–24. [PubMed: 10855596]

[8]. Saczynski JS, Marcantonio ER, Quach L, Fong TG, Gross A, Inouye SK, et al. Cognitive trajectories after postoperative delirium. N Engl J Med. 2012;367:30–9. [PubMed: 22762316]

[9]. Marcantonio ER, Goldman L, Mangione CM, Ludwig LE, Muraca B, Haslauer CM, et al. A clinical prediction rule for delirium after elective noncardiac surgery. JAMA. 1994;271:134–9. [PubMed: 8264068]

[10]. Robinson TN, Raeburn CD, Tran ZV, Angles EM, Brenner LA, Moss M. Postoperative delirium in the elderly: risk factors and outcomes. Ann Surg. 2009;249:173–8. [PubMed: 19106695]

[11]. Gou RY, Hshieh TT, Marcantonio ER, Cooper Z, Jones RN, Travison TG, et al. One-Year Medicare Costs Associated With Delirium in Older Patients Undergoing Major Elective Surgery. JAMA Surg. 2021;156:430–42.

[12]. Davis DH, Muniz Terrera G, Keage H, Rahkonen T, Oinas M, Matthews FE, et al. Delirium is a strong risk factor for dementia in the oldest-old: a population-based cohort study. Brain. 2012;135:2809–16. [PubMed: 22879644]

[13]. Ags/Nia Delirium Conference Writing Group PC, Faculty. The American Geriatrics Society/National Institute on Aging Bedside-to-Bench Conference: Research Agenda on Delirium in Older Adults. J Am Geriatr Soc. 2015;63:843–52. [PubMed: 25834932]

[14]. Fong TG, Davis D, Growdon ME, Albuquerque A, Inouye SK. The interface between delirium and dementia in elderly adults. Lancet Neurol. 2015;14:823–32. [PubMed: 26139023]

[15]. Fong TG, Jones RN, Shi P, Marcantonio ER, Yap L, Rudolph JL, et al. Delirium accelerates cognitive decline in Alzheimer disease. Neurology. 2009;72:1570–5. [PubMed: 19414723]

[16]. Binder LI, Frankfurter A, Rebhun LI. The distribution of tau in the mammalian central nervous system. J Cell Biol. 1985;101:1371–8. [PubMed: 3930508]

[17]. Dujardin S, Colin M, Buee L. Invited review: Animal models of tauopathies and their implications for research/translation into the clinic. Neuropathol Appl Neurobiol. 2015;41:59–80. [PubMed: 25428793]

[18]. Wang Y, Mandelkow E. Tau in physiology and pathology. Nat Rev Neurosci. 2016;17:5–21. [PubMed: 26631930]

[19]. Ittner A, Ittner LM. Dendritic Tau in Alzheimer's Disease. Neuron. 2018;99:13–27. [PubMed: 30001506]

[20]. Balczon R, Lin MT, Lee JY, Abbasi A, Renema P, Voth SB, et al. Pneumonia initiates a tauopathy. FASEB J. 2021;35:e21807. [PubMed: 34384141]

[21]. Chang CW, Shao E, Mucke L. Tau: Enabler of diverse brain disorders and target of rapidly evolving therapeutic strategies. Science. 2021;371.

[22]. Querfurth HW, LaFerla FM. Alzheimer's disease. N Engl J Med. 2010;362:329–44. [PubMed: 20107219]

[23]. Holtzman DM, Carrillo MC, Hendrix JA, Bain LJ, Catafau AM, Gault LM, et al. Tau: From research to clinical development. Alzheimers Dement. 2016;12:1033–9. [PubMed: 27154059]

[24]. Tatebe H, Kasai T, Ohmichi T, Kishi Y, Kakeya T, Waragai M, et al. Quantification of plasma phosphorylated tau to use as a biomarker for brain Alzheimer pathology: pilot case-control studies including patients with Alzheimer's disease and down syndrome. Mol Neurodegener. 2017;12:63. [PubMed: 28866979]

[25]. Mielke MM, Hagen CE, Xu J, Chai X, Vemuri P, Lowe VJ, et al. Plasma phospho-tau181 increases with Alzheimer's disease clinical severity and is associated with tau- and amyloid-positron emission tomography. Alzheimers Dement. 2018;14:989–97. [PubMed: 29626426]

[26]. Janelidze S, Mattsson N, Palmqvist S, Smith R, Beach TG, Serrano GE, et al. Plasma P-tau181 in Alzheimer's disease: relationship to other biomarkers, differential diagnosis, neuropathology and longitudinal progression to Alzheimer's dementia. Nat Med. 2020;26:379–86. [PubMed: 32123385]

[27]. Thijssen EH, La Joie R, Wolf A, Strom A, Wang P, Iaccarino L, et al. Diagnostic value of plasma phosphorylated tau181 in Alzheimer's disease and frontotemporal lobar degeneration. Nat Med. 2020;26:387–97. [PubMed: 32123386]

[28]. Suarez-Calvet M, Karikari TK, Ashton NJ, Lantero Rodriguez J, Mila-Aloma M, Gispert JD, et al. Novel tau biomarkers phosphorylated at T181, T217 or T231 rise in the initial stages of the preclinical Alzheimer's continuum when only subtle changes in Abeta pathology are detected. EMBO Mol Med. 2020;12:e12921. [PubMed: 33169916]

[29]. Palmqvist S, Insel PS, Stomrud E, Janelidze S, Zetterberg H, Brix B, et al. Cerebrospinal fluid and plasma biomarker trajectories with increasing amyloid deposition in Alzheimer's disease. EMBO Mol Med. 2019;11:e11170. [PubMed: 31709776]

[30]. Palmqvist S, Janelidze S, Quiroz YT, Zetterberg H, Lopera F, Stomrud E, et al. Discriminative Accuracy of Plasma Phospho-tau217 for Alzheimer Disease vs Other Neurodegenerative Disorders. JAMA. 2020;324:772–81. [PubMed: 32722745]

[31]. Janelidze S, Berron D, Smith R, Strandberg O, Proctor NK, Dage JL, et al. Associations of Plasma Phospho-Tau217 Levels With Tau Positron Emission Tomography in Early Alzheimer Disease. JAMA neurology. 2021;78:149–56. [PubMed: 33165506]

[32]. Thijssen EH, La Joie R, Strom A, Fonseca C, Iaccarino L, Wolf A, et al. Plasma phosphorylated tau 217 and phosphorylated tau 181 as biomarkers in Alzheimer's disease and frontotemporal lobar degeneration: a retrospective diagnostic performance study. Lancet Neurol. 2021;20:739–52. [PubMed: 34418401]

[33]. Liang F, Baldyga K, Quan Q, Khatri A, Choi S, Wiener-Kronish J, et al. Preoperative Plasma Tau-PT217 and Tau-PT181 Are Associated With Postoperative Delirium. Ann Surg. 2022.

[34]. McKay TB, Qu J, Liang F, Mueller A, Wiener-Kronish J, Xie Z, et al. Tau as a serum biomarker of delirium after major cardiac surgery: a single centre case-control study. Br J Anaesth. 2022;129:e13–e6. [PubMed: 35465951]

[35]. Vossel KA, Xu JC, Fomenko V, Miyamoto T, Suberbielle E, Knox JA, et al. Tau reduction prevents Abeta-induced axonal transport deficits by blocking activation of GSK3beta. J Cell Biol. 2015;209:419–33. [PubMed: 25963821]

[36]. Yuan A, Kumar A, Peterhoff C, Duff K, Nixon RA. Axonal transport rates in vivo are unaffected by tau deletion or overexpression in mice. J Neurosci. 2008;28:1682–7. [PubMed: 18272688]

[37]. Tai C, Chang CW, Yu GQ, Lopez I, Yu X, Wang X, et al. Tau Reduction Prevents Key Features of Autism in Mouse Models. Neuron. 2020;106:421–37 e11. [PubMed: 32126198]

[38]. Gheyara AL, Ponnusamy R, Djukic B, Craft RJ, Ho K, Guo W, et al. Tau reduction prevents disease in a mouse model of Dravet syndrome. Ann Neurol. 2014;76:443–56. [PubMed: 25042160]

[39]. Roberson ED, Scearce-Levie K, Palop JJ, Yan F, Cheng IH, Wu T, et al. Reducing endogenous tau ameliorates amyloid beta-induced deficits in an Alzheimer's disease mouse model. Science. 2007;316:750–4. [PubMed: 17478722]

[40]. Das M, Maeda S, Hu B, Yu GQ, Guo W, Lopez I, et al. Neuronal levels and sequence of tau modulate the power of brain rhythms. Neurobiol Dis. 2018;117:181–8. [PubMed: 29859869]

[41]. Morris M, Hamto P, Adame A, Devidze N, Masliah E, Mucke L. Age-appropriate cognition and subtle dopamine-independent motor deficits in aged tau knockout mice. Neurobiol Aging. 2013;34:1523–9. [PubMed: 23332171]

[42]. Ittner LM, Ke YD, Delerue F, Bi M, Gladbach A, van Eersel J, et al. Dendritic function of tau mediates amyloid-beta toxicity in Alzheimer's disease mouse models. Cell. 2010;142:387–97. [PubMed: 20655099]

[43]. DeVos SL, Goncharoff DK, Chen G, Kebodeaux CS, Yamada K, Stewart FR, et al. Antisense reduction of tau in adult mice protects against seizures. J Neurosci. 2013;33:12887–97. [PubMed: 23904623]

[44]. DeVos SL, Miller RL, Schoch KM, Holmes BB, Kebodeaux CS, Wegener AJ, et al. Tau reduction prevents neuronal loss and reverses pathological tau deposition and seeding in mice with tauopathy. Sci Transl Med. 2017;9.

[45]. Sotiropoulos I, Galas MC, Silva JM, Skoulakis E, Wegmann S, Maina MB, et al. Atypical, non-standard functions of the microtubule associated Tau protein. Acta Neuropathol Commun. 2017;5:91. [PubMed: 29187252]

[46]. Bi M, Gladbach A, van Eersel J, Ittner A, Przybyla M, van Hummel A, et al. Tau exacerbates excitotoxic brain damage in an animal model of stroke. Nat Commun. 2017;8:473. [PubMed: 28883427]

[47]. Kim K, Wang X, Ragonnaud E, Bodogai M, Illouz T, DeLuca M, et al. Therapeutic B-cell depletion reverses progression of Alzheimer's disease. Nat Commun. 2021;12:2185. [PubMed: 33846335]

[48]. Huang LT, Zhang CP, Wang YB, Wang JH. Association of Peripheral Blood Cell Profile With Alzheimer's Disease: A Meta-Analysis. Front Aging Neurosci. 2022;14:888946. [PubMed: 35601620]

[49]. Xiong LL, Xue LL, Du RL, Niu RZ, Chen L, Chen J, et al. Single-cell RNA sequencing reveals B cell-related molecular biomarkers for Alzheimer's disease. Exp Mol Med. 2021;53:1888–901. [PubMed: 34880454]

[50]. Hopkins S, Scorneaux B, Huang Z, Murray MG, Wring S, Smitley C, et al. SCY-635, a novel nonimmunosuppressive analog of cyclosporine that exhibits potent inhibition of hepatitis C virus RNA replication in vitro. Antimicrob Agents Chemother. 2010;54:660–72. [PubMed: 19933795]

[51]. Bobardt M, Chatterji U, Lim P, Gawlik K, Gallay P. Both Cyclophilin Inhibitors and Direct-Acting Antivirals Prevent PKR Activation in HCV-Infected Cells. Open Virol J. 2014;8:1–8. [PubMed: 24799968]

[52]. Zhang C, Zhang Y, Shen Y, Zhao G, Xie Z, Dong Y. Anesthesia/Surgery Induces Cognitive Impairment in Female Alzheimer's Disease Transgenic Mice. J Alzheimers Dis. 2017;57:505–18. [PubMed: 28269788]

[53]. Evered L, Silbert B, Knopman DS, Scott DA, DeKosky ST, Rasmussen LS, et al. Recommendations for the Nomenclature of Cognitive Change Associated with Anaesthesia and Surgery-2018. Anesthesiology. 2018;129:872–9. [PubMed: 30325806]

[54]. Peng M, Zhang C, Dong Y, Zhang Y, Nakazawa H, Kaneki M, et al. Battery of behavioral tests in mice to study postoperative delirium. Scientific reports. 2016;6:29874. [PubMed: 27435513]

[55]. Yang S, Gu C, Mandeville, Dong Y, Esposito E, Zhang Y, Yang G, Shen Y, Fu X, Eng H and Xie Z Aneshethesia and surgery impair blood-brain barrier and cogntive function in mice. Frontiers in Immunology. 2017;8. [PubMed: 28144241]

[56]. Liufu N, Liu L, Shen S, Jiang Z, Dong Y, Wang Y, et al. Anesthesia and surgery induce age-dependent changes in behaviors and microbiota. Aging (Albany NY). 2020;12:1965–86. [PubMed: 31974315]

[57]. Ren X, Zhang S, Yang Y, Song A, Liang F, Zhang Y, et al. Ketamine Induces Delirium-Like Behavior and Interferes With Endosomal Tau Trafficking. Anesth Analg. 2022.

[58]. Jiang Z, Liang F, Zhang Y, Dong Y, Song A, Zhu X, et al. Urinary Catheterization Induces Delirium-Like Behavior Through Glucose Metabolism Impairment in Mice. Anesth Analg. 2022;135:641–52. [PubMed: 35389369]

[59]. Moller JT, Cluitmans P, Rasmussen LS, Houx P, Rasmussen H, Canet J, et al. Long-term postoperative cognitive dysfunction in the elderly ISPOCD1 study. ISPOCD investigators. International Study of Post-Operative Cognitive Dysfunction. Lancet. 1998;351:857–61. [PubMed: 9525362]

[60]. Voigt Hansen M, Rasmussen LS, Jespersgaard C, Rosenberg J, Gogenur I. There is no association between the circadian clock gene HPER3 and cognitive dysfunction after noncardiac surgery. Anesth Analg. 2012;115:379–85. [PubMed: 22543063]

[61]. Rasmussen LS, Larsen K, Houx P, Skovgaard LT, Hanning CD, Moller JT. The assessment of postoperative cognitive function. Acta Anaesthesiol Scand. 2001;45:275–89. [PubMed: 11207462]

[62]. Bai P, Mondal P, Bagdasarian FA, Rani N, Liu Y, Gomm A, et al. Development of a potential PET probe for HDAC6 imaging in Alzheimer's disease. Acta Pharm Sin B. 2022;12:3891–904. [PubMed: 36213537]

[63]. Bai P, Lan Y, Patnaik D, Wang H, Liu Y, Chen Z, et al. Design, Synthesis, and Evaluation of Thienodiazepine Derivatives as Positron Emission Tomography Imaging Probes for Bromodomain and Extra-Terminal Domain Family Proteins. J Med Chem. 2021;64:14745–56. [PubMed: 34549949]

[64]. Behrendt R, White P, Offer J. Advances in Fmoc solid-phase peptide synthesis. J Pept Sci. 2016;22:4–27. [PubMed: 26785684]

[65]. Teixeira A, Benckhuijsen WE, de Koning PE, Valentijn AR, Drijfhout JW. The use of DODT as a non-malodorous scavenger in Fmoc-based peptide synthesis. Protein Pept Lett. 2002;9:379–85. [PubMed: 12370025]

[66]. Sandoval H, Kodali S, Wang J. Regulation of B cell fate, survival, and function by mitochondria and autophagy. Mitochondrion. 2018;41:58–65. [PubMed: 29175010]

[67]. Balczon R, Morrow KA, Zhou C, Edmonds B, Alexeyev M, Pittet JF, et al. Pseudomonas aeruginosa infection liberates transmissible, cytotoxic prion amyloids. FASEB J. 2017;31:2785–96. [PubMed: 28314768]

[68]. Mattsson-Carlgren N, Janelidze S, Bateman RJ, Smith R, Stomrud E, Serrano GE, et al. Soluble P-tau217 reflects amyloid and tau pathology and mediates the association of amyloid with tau. EMBO Mol Med. 2021;13:e14022. [PubMed: 33949133]

[69]. Gonzalez-Ortiz F, Turton M, Kac PR, Smirnov D, Premi E, Ghidoni R, et al. Brain-derived tau: a novel blood-based biomarker for Alzheimer's disease-type neurodegeneration. Brain. 2023;146:1152–65. [PubMed: 36572122]

[70]. Feng W, Zhang Y, Ding S, Chen S, Wang T, Wang Z, et al. B lymphocytes ameliorate Alzheimer's disease-like neuropathology via interleukin-35. Brain Behav Immun. 2022;108:16–31. [PubMed: 36427805]

[71]. Casola S, Otipoby KL, Alimzhanov M, Humme S, Uyttersprot N, Kutok JL, et al. B cell receptor signal strength determines B cell fate. Nat Immunol. 2004;5:317–27. [PubMed: 14758357]

[72]. Nicolli A, Basso E, Petronilli V, Wenger RM, Bernardi P. Interactions of cyclophilin with the mitochondrial inner membrane and regulation of the permeability transition pore, and cyclosporin A-sensitive channel. J Biol Chem. 1996;271:2185–92. [PubMed: 8567677]

[73]. Marchetti P, Castedo M, Susin SA, Zamzami N, Hirsch T, Macho A, et al. Mitochondrial permeability transition is a central coordinating event of apoptosis. J Exp Med. 1996;184:1155–60. [PubMed: 9064332]

[74]. Lin J, Shen F, Lu J, Liang F, Zhang Y, Xie Z, et al. WS635 Attenuates the Anesthesia/Surgery-Induced Cognitive Impairment in Mice. Front Aging Neurosci. 2021;13:688587. [PubMed: 34366827]

[75]. Dam T, Boxer AL, Golbe LI, Hoglinger GU, Morris HR, Litvan I, et al. Safety and efficacy of anti-tau monoclonal antibody gosuranemab in progressive supranuclear palsy: a phase 2, randomized, placebo-controlled trial. Nat Med. 2021;27:1451–7. [PubMed: 34385707]

[76]. Zhang J, Dong Y, Huang L, Xu X, Liang F, Soriano SG, Zhang Y and Xie Z Interaction of Tau, IL-6 and mitochondria on synapse and cognition following sevoflurane anesthesia in young mice. Brain, Behavior, & Immunity - Health. 2020;8:1–18.

[77]. Vasunilashorn SM, Lunardi N, Newman JC, Crosby G, Acker L, Abel T, et al. Preclinical and translational models for delirium: Recommendations for future research from the NIDUS delirium network. Alzheimers Dement. 2023.

[78]. Yang L, Ding W, Dong Y, Chen C, Zeng Y, Jiang Z, Gan S, You Z, Dai J, Chen Z, Zhu S, Chen L, Shen S, Mao J and Xie Z Electroacupuncture attenuates surgical pain-induced delirium-like behavior in mice via remodeling of gut microbiota and dendritic spine. Frontiers in Immunology. 2022;In Press.

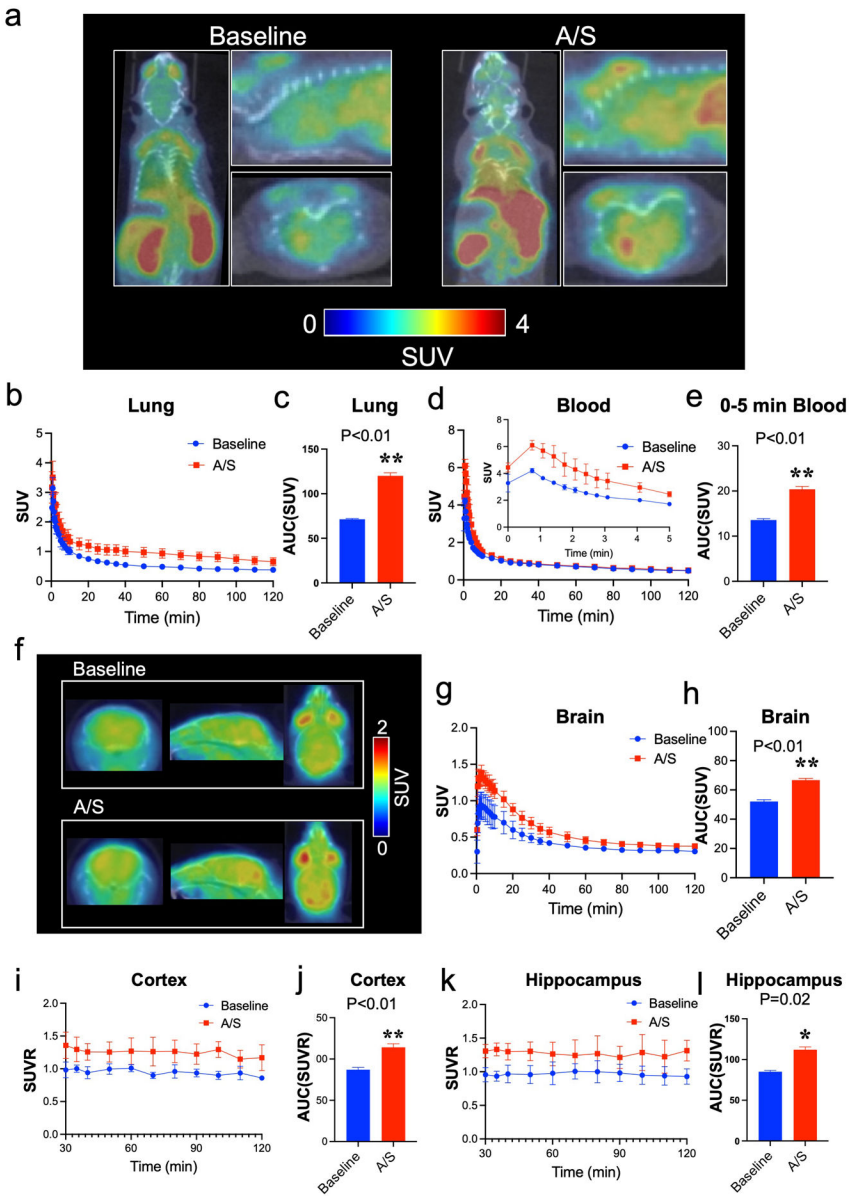

Fig. 1. PET study of A/S-induced increases in Tau-PT217 amounts in lungs, blood, and brain of mice.

a. Representative PET images of [^{18}F]Flortaucipir focus on the whole body of the mouse for up to 120 minutes. Time-activity curves of [^{18}F]Flortaucipir in the lungs (**b** and **c**) and blood (**d** and **e**) show significant differences in the distribution of [^{18}F]Flortaucipir in lungs and blood between the time before A/S (baseline) and the time after A/S in the mice. **f**. Representative PET images of [18F]Flortaucipir focus on the mouse brain tissues (0-120 minutes; axial, sagittal, and coronal). Time-activity curves of [^{18}F]Flortaucipir in the whole brain (**g** and **h**) between baseline and A/S in the mice. Standardized uptake value ratio (SUVR) of [^{18}F]Flortaucipir in the cortex (**i** and **j**) and hippocampus (**k** and **l**), showing a significant difference of [^{18}F]Flortaucipir brain uptake between baseline and A/S in the mice. Cerebellar gray matter was used as a reference region to yield SUVR for [^{18}F]Flortaucipir. N = 4 mice in each group. Student's t-test was used to analyze the data

presented in c, e, h, j, and i. The P values refer to the difference of [^{18}F]Flortaucipir uptake between the baseline and the A/S in the mice. Error bar indicates standard deviation. PET, positron emission tomography; A/S, anesthesia/surgery; Tau-PT217, Tau phosphorylated at threonine 217; TACs, time activity curves; AUC, area under each TAC; SUV, standardized uptake value; SUVR, standardized uptake value ratio.

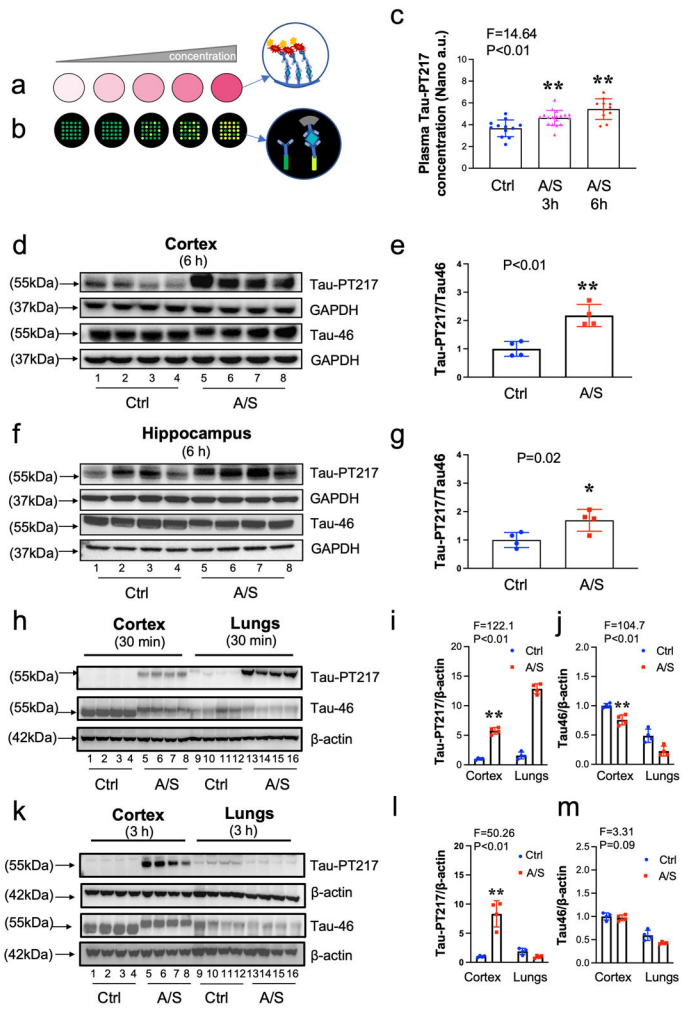

Fig. 2. A/S increased Tau-PT217 amounts in the lungs, blood, and brain of mice.

a. Classical immunoassay monitors absorbance signal due to the increased amount of chromogen as the analyte concentration increases. **b**. Nanoneedle technology detecting spectrum shift from individual nanoneedles originated from additional mass deposition on each nanoneedle, forming an antibody-antigen sandwich complex. **c**. Low concentrations of plasma Tau-PT217 were detected with nanoneedle technology. Significant increases in Tau-PT217 amount were observed 3 and 6 h after the A/S compared to the control condition in mice. Quantitative western blot showing A/S increased Tau-PT217 amount in the cortex (**d** and **e**) and hippocampus (**f** and **g**) compared to control condition in the mice. Comparisons of A/S-induced increases in Tau-PT217 amounts between lungs and brain tissues (cortex) 30 minutes following A/S (**h, i** and **j**), demonstrating that the A/S caused more increases of Tau-PT217 and lesser decreases of total Tau in lungs compared to the cortex of mice. Comparisons of A/S-induced increases in Tau-PT217 amounts between lungs and brain tissues (cortex) 3 hours following A/S (**k, l,** and **m**), demonstrating that the A/S caused more increases of Tau-PT217 in the cortex compared to lungs of mice. N = 4 mice in each group, as demonstrated in each panel of the figure. One-way ANOVA and the post-hoc analysis with Bonferroni were used to analyze the data presented in c. Student's t-test was used to

analyze the data presented in e and g. Two-way ANOVA and the post-hoc analysis with Bonferroni were used to analyze the data presented in i, j. l and m. The P values refer to the differences of Tau-PT217 between the control condition and A/S in the mice. Error bar indicates standard deviation. A/S, anesthesia/surgery; Tau-PT217, Tau phosphorylated at threonine 217.

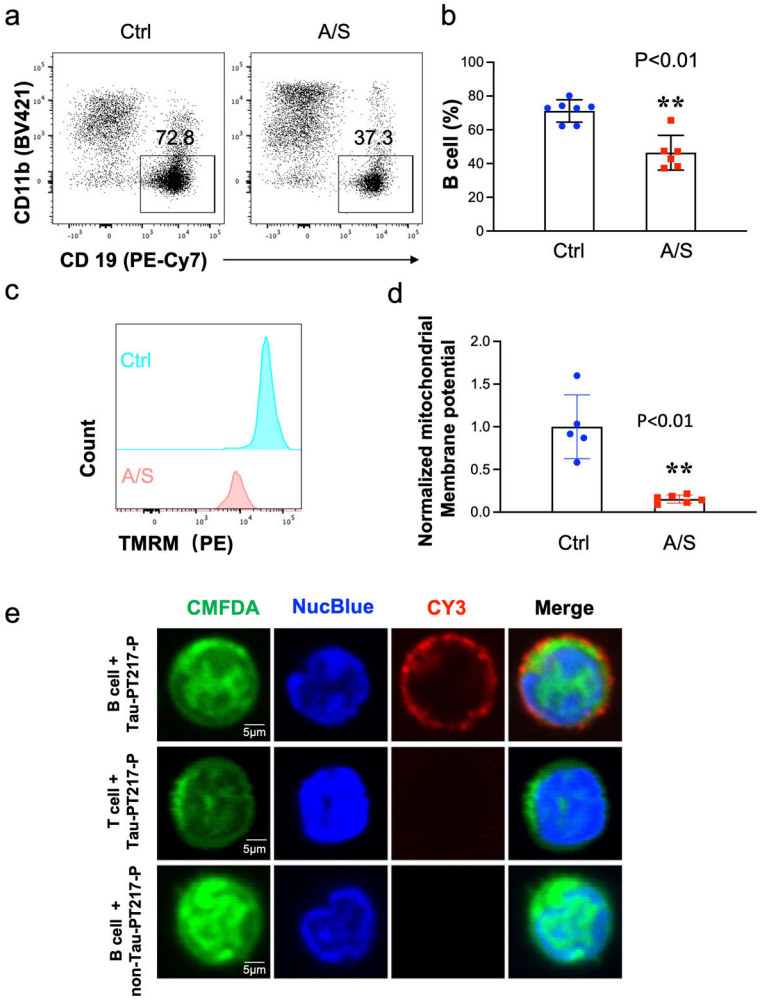

Fig. 3. A/S decreased the percentage of blood B cells in aged mice.

Flow cytometry showed that A/S decreased the percentage of blood B cells (live CD45+ CD3− LY6G− CD11b− CD19+) compared to the control condition (**a** and **b**). Flow cytometry also showed that A/S decreased mitochondrial membrane potential (represented by TRAM amounts) of B cells in the blood of mice (**c** and **d**). **e**. Confocal microscope images showed that B cells (upper panel), but not T cells (middle panel), could bind to the 14 amino acid peptide containing Tau-PT217, but not the 14 amino acid peptide without containing Tau-PT217 (bottom panel). N = 5 - 7 mice in each group, as demonstrated in each panel of the figure. The Student's t-test was used to analyze the data presented in b and d. The P values refer to the differences in the numbers of B cells or mitochondrial membrane potential between the control condition and A/S in the mice. Error bar indicates standard deviation. Tau-PT217, Tau phosphorylated at threonine 217; A/S, anesthesia, and surgery; TMRM, tetramethylrhodamine methyl ester; DAPI, 4',6-diamidino-2-phenylindole.

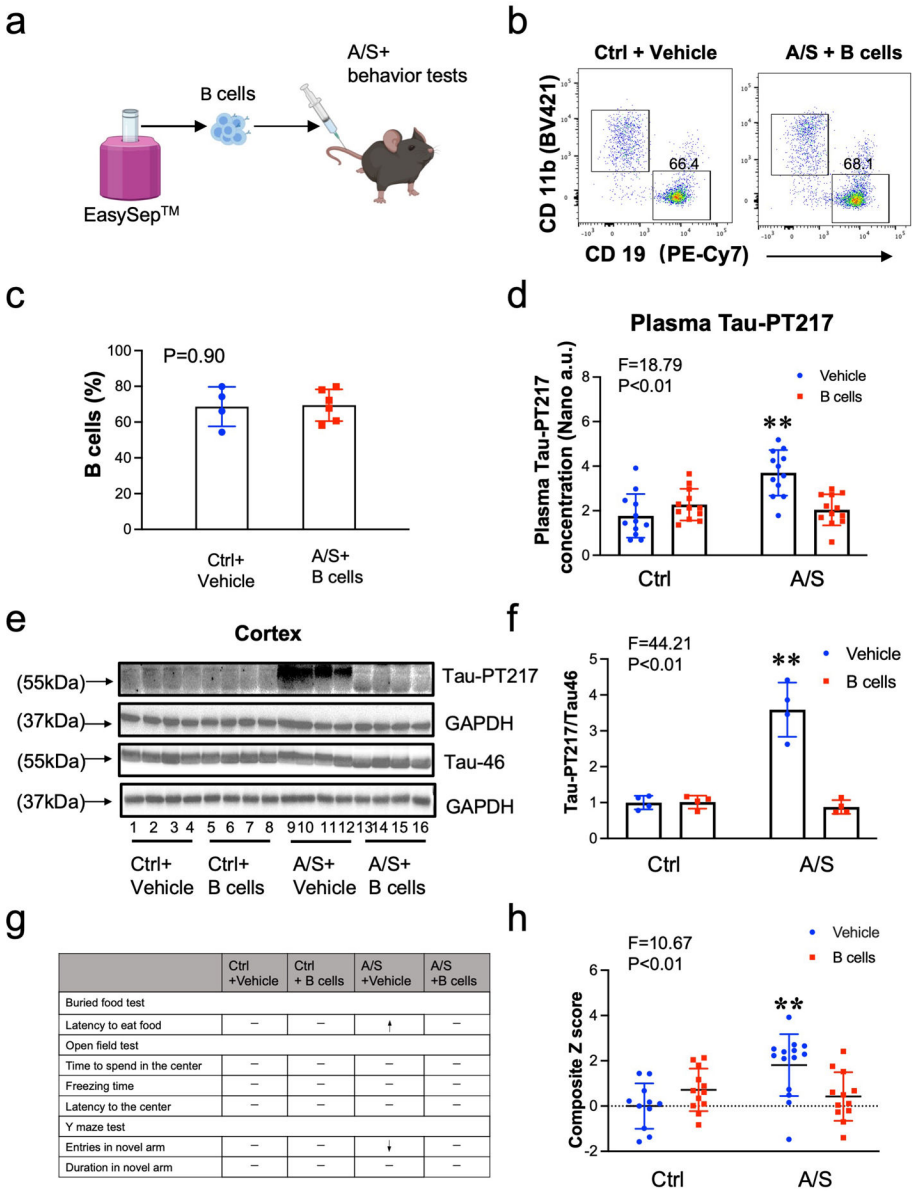

	Ctrl +Vehicle	Ctrl + B cells	A/S +Vehicle	A/S +B cells
Buried food test				
Latency to eat food	–	–	↑	–
Open field test				
Time to spend in the center	–	–	–	–
Freezing time	–	–	–	–
Latency to the center	–	–	–	–
Y maze test				
Entries in novel arm	–	–	↓	–
Duration in novel arm	–	–	–	–

Fig. 4. Treatment with B cells mitigated the A/S-induced delirium-like behaviors in mice.

a. Experimental scheme: B cells (6 x 10^6) were negatively sorted from donor mice (4 months old female mice) using EasySep™ and injected (2 x 10^6) into recipient-aged mice, followed by control condition and A/S, and behavioral tests. **b**. Representative flow cytograms of B cells in the blood of recipient mice. **c**. B cell amounts in the mice with control condition plus vehicle treatment and the mice with A/S plus B cell treatment. **d**. B cell treatment attenuated the A/S-induced increases in blood Tau-PT217 amounts in the aged mice. Quantitative western blot showing that B cell treatment attenuated the A/S-induced increases in cortex Tau-PT217 in the mice (**e** and **f**). Treatment with B cells mitigated the A/S-induced delirium-like behaviors in mice demonstrated in individual tests (**g**) and composite Z score (**h**). N = 10 - 12 mice in each group of behavioral test, and N = 4 - 6 mice in each flow cytometry, nanoneedle, and western blot study as demonstrated in each

panel of the figure. The Student's t-test was used to analyze the data presented in c. Two-way ANOVA and the post-hoc analysis with Bonferroni were used to analyze the data presented in d, f, and h. The P values refer to the difference in B cell amounts, Tau-PT217 amounts, and Z score between the control condition and A/S in the mice. Error bar indicates standard deviation. Tau-PT217, Tau phosphorylated at threonine 217; A/S, anesthesia and surgery.

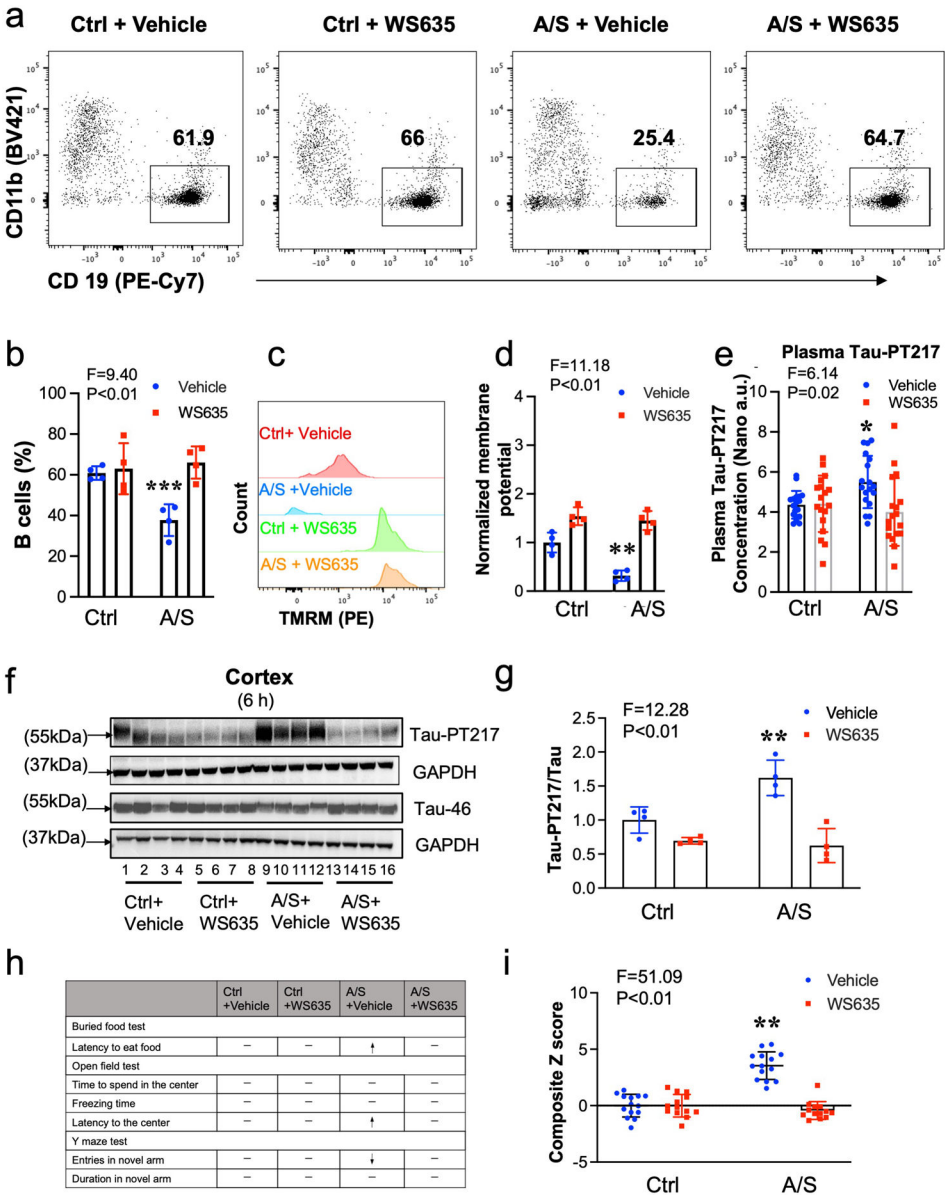

	Ctrl +Vehicle	Ctrl +WS635	A/S +Vehicle	A/S +WS635
Buried food test				
Latency to eat food	–	–	+	–
Open field test				
Time to spend in the center	–	–	–	–
Freezing time	–	–	–	–
Latency to the center	–	–	+	–
Y maze test				
Entries in novel arm	–	–	+	–
Duration in novel arm	–	–	–	–

Fig. 5. WS635 mitigated the A/S-induced changes in B cells, Tau-PT217 amounts, and delirium-like behaviors in mice.

Flow cytometry showed that WS635 attenuated the A/S-induced reductions in blood B cells (**a** and **b**) and mitochondrial membrane potential (represented by TRAM) (**c** and **d**). Nanoneedle analysis showed that WS635 attenuated the A/S-induced increases in blood Tau-PT217 amounts in the mice (**e**). Quantitative western blot showing that WS635 attenuated the A/S-induced increases in cortex Tau-PT217 amounts in the mice (**f** and **g**). WS635 rescued the A/S-induced delirium-like behaviors in mice, demonstrated in individual test (**h**) and composite Z score (**i**) in the mice. N = 10 - 12 mice in each group of behavioral test, and N = 4 - 6 mice in each group in flow cytometry, nanoneedle, and western blot study as demonstrated in each panel of the figure. Two-way ANOVA and the post-hoc analysis with Bonferroni were used to analyze the data presented in b, d, e, g, and i. The P values refer to the differences in B cells, Tau-PT217, and Z scores between the control condition and

A/S in the mice. Error bar indicates standard deviation. Tau-PT217, Tau phosphorylated at threonine 217; A/S, anesthesia, and surgery; TMRM, tetramethylrhodamine methyl ester.

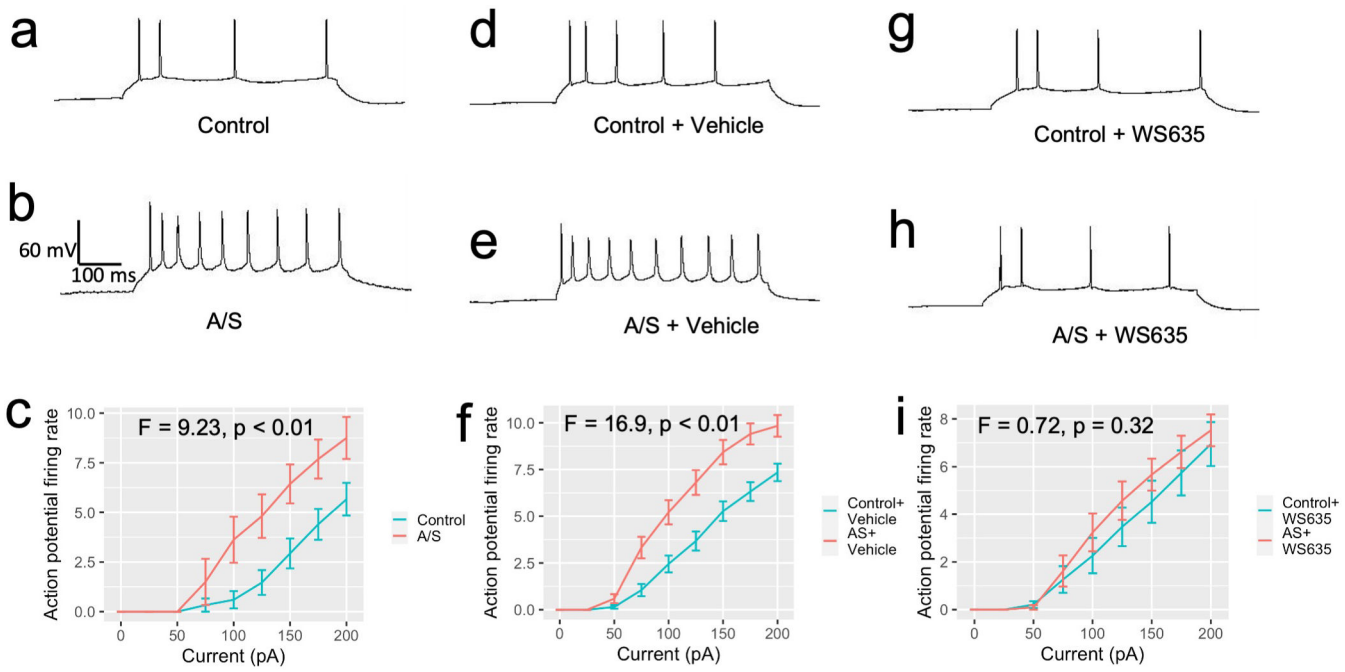

Fig. 6. WS635 mitigated the A/S-induced ACC neuronal excitability of the aged mice.

The whole cell patch-clamp recording sample trace of neurons action potential firing rate with 150 pA of current injection in ACC slice harvested from the aged mice following the control condition (**a**) and the aged mice following the A/S (**b**). **c**. Action potential firing rates of ACC neurons with different amounts of current injection were higher in mice that underwent the A/S compared to control condition (mixed two-way ANOVA, $F = 9.23$, $p < 0.01$, control: $n = 16$, 3 mice, A/S: $n = 16$, 4 mice). The whole cell patch-clamp recording sample trace of neurons action potential firing rate with 150 pA of current injection in ACC slice harvested from the aged mice following the control condition (**d**) and the aged mice following the A/S (**e**) pretreated with the vehicle of WS635. **f**. The action potential firing rates of ACC neurons still increased after the A/S in the ACC slice of the aged mice pretreated with vehicle (mixed two-way ANOVA, $F = 16.9$, $p < 0.01$, control + vehicle: $n = 40$, 5 mice, A/S + vehicle: $n = 37$, 5 mice). The whole cell patch-clamp recording sample trace of neurons action potential firing rate with 150 pA of current injection in ACC slice harvested from the aged mice following the control condition (**g**) and the aged mice following the A/S (**h**) pretreated with WS635. **i**. The action potential firing rates of ACC neurons did not increase after the A/S compared to control condition in the aged mice pretreated with WS635 (mixed two-way ANOVA, $F = 0.72$, $p = 0.32$, control + WS635: $n = 19$, 3 mice, A/S + WS635: $n = 21$, 3 mice). Tau-PT217, Tau phosphorylated at threonine 217; A/S, anesthesia, and surgery; ACC, anterior cingulate cortex.

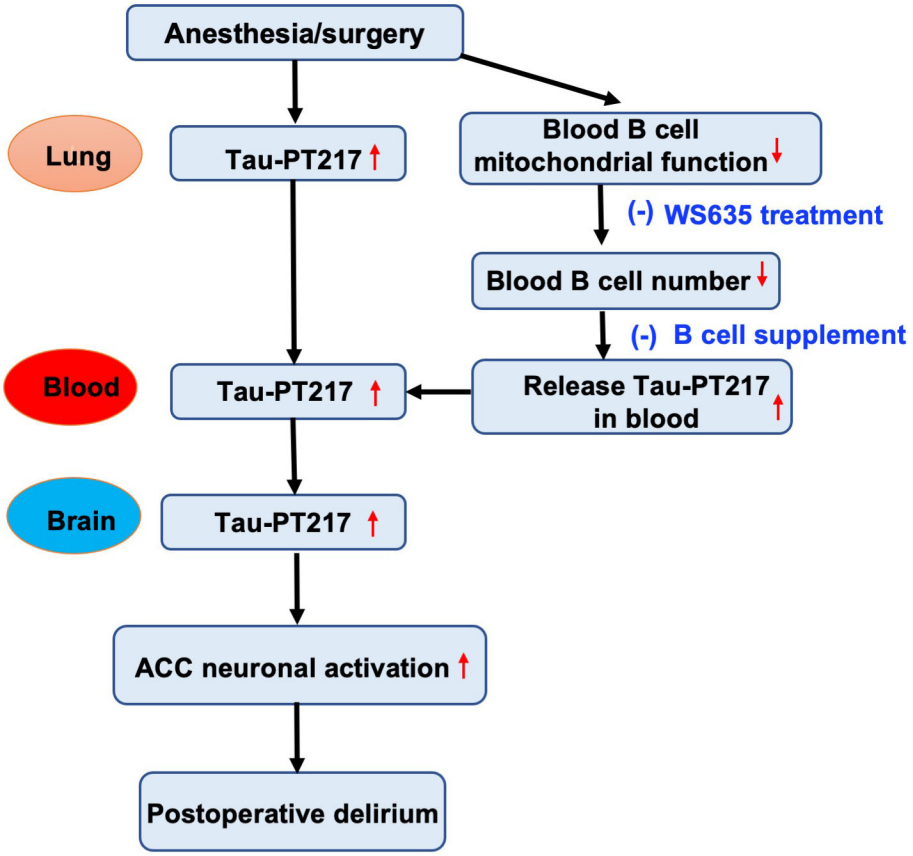

Fig. 7. The hypothesized pathway of the acutely increased blood Tau-PT217 and postoperative delirium-like behavior in aged mice.

The anesthesia/surgery increased the generation of Tau-PT217 potentially in the lungs of aged mice, leading to increased blood Tau-PT217 amounts in the mice. The mitochondrial function in B cells was impaired after the A/S, leading to fewer B cells in the blood. Moreover, B cells bind to Tau-PT217. Thus, the reductions in blood B cells result in the release of Tau-PT217, leading to more Tau-PT217 in the blood of mice. The acutely increased blood Tau-PT217 may then enter the brain, leading to increased Tau-217 amounts in the cortex and hippocampus, finally leading to an increased action potential firing rate in ACC of aged mice and postoperative delirium-like behavior in the mice. Tau-PT217, Tau phosphorylated at threonine 217; A/S, anesthesia, and surgery; ACC, anterior cingulate cortex.